EURASIP Journal on
Wireless Communications and Networking
a SpringerOpen Journal

RESEARCH Open Access

State modelling of the land mobile propagation channel for dual-satellite systems

Daniel Arndt[1*], Alexander Ihlow[1], Thomas Heyn[2], Albert Heuberger[2], Roberto Prieto-Cerdeira[3] and Ernst Eberlein[2]

Abstract

The quality of service of mobile satellite reception can be improved by using multi-satellite diversity (angle diversity). The recently finalised MiLADY project targeted therefore on the evaluation and modelling of the multi-satellite propagation channel for land mobile users with focus on broadcasting applications. The narrowband model combines the parameters from two measurement campaigns: In the U.S. the power levels of the Satellite Digital Audio Radio Services were recorded with a high sample rate to analyse fast and slow fading effects in great detail. In a complementary campaign signals of Global Navigation Satellite Systems (GNSS) were analysed to obtain information about the slow fading correlation for almost any satellite constellation. The new channel model can be used to generate time series for various satellite constellations in different environments. This article focuses on realistic state sequence modelling for angle diversity, confining on two satellites. For this purpose, different state modelling methods providing a joint generation of the states 'good good', 'good bad', 'bad good' and 'bad bad' are compared. Measurements and re-simulated data are analysed for various elevation combinations and azimuth separations in terms of the state probabilities, state duration statistics, and correlation coefficients. The finally proposed state model is based on semi-Markov chains assuming a log-normal state duration distribution.

Keywords: Land mobile satellite, Statistical propagation model, Satellite diversity, Markov chain, Semi-Markov chain

1 Introduction

Satellites play an important role in today's commercial broadcasting systems. In cooperation with terrestrial repeaters they can ensure uninterrupted service of multimedia content (e.g. audio and video streaming) to stationary, portable, and mobile receivers. However, in case of mobile reception fading regularly disrupts the signal transmission due to shadowing or blocking objects between satellite and receiver. To mitigate these fading effects, diversity techniques such as angle diversity (multiple satellites) and time diversity (interleaving) are attractive. For link-level studies of the land mobile satellite (LMS) channel, statistical channel models are frequently used that are able to generate timeseries of the received fading signal. Statistical LMS channel models describe several fading processes of the received signal: slow variations of the signal are caused by obstacles between the satellite and the receiver, which induce varying shadowing conditions of the direct signal component. Fast signal variations are caused by multipath effects due to static or moving scatterers in the vicinity of the mobile terminal. For short time periods these two components (*slow and fast variations*) are usually modelled by a stationary stochastic processes, e.g., as a Loo-distributed fading signal [1]. For longer time periods the received signal can not assumed to be stationary. Therefore, statistical LMS channel models describe different receive states to assess the large dynamic range of the received signal. The states correspond to slow varying environmental conditions (e.g. line of trees, buildings, line-of-sight (LOS)) in the transmission path. Traditional LMS channel models simulate series of three states ('line-of-sight', 'shadowed', and 'blocked') or two states ('good' state and 'bad' state) by using Markov or semi-Markov concepts.

While several LMS channel models for single-satellite systems are already available and consolidated [2-4], models for multi-satellites systems are of ongoing interest for modern transmission standards, e.g. DVB-SH [5].

*Correspondence: daniel.arndt@tu-ilmenau.de
[1] Ilmenau University of Technology, Ilmenau, Germany
Full list of author information is available at the end of the article

Early studies on multi-satellite transmission were carried out in 1992. Based on circular scans of fisheye-camera pictures in different environments an empirical model was developed describing the correlation coefficient between two satellite signals depending on their azimuth separation [6]. In 1996 a statistical channel model for two correlated satellites based on first-order Markov chains was developed [7]. The state sequence generation is based on state transition probabilities of two independent satellites. Both satellites are combined by a state correlation parameter which can be taken from empirical models. Due to its simplicity this modelling approach is frequently used today. However, first-order Markov chains have limitations in state duration modelling, as their state durations follow an exponential distribution. Studies in [8-10] found that this condition does not hold for the LMS channel. Nevertheless, a correct state duration modelling is of high interest for the optimal configuration of physical layer and link layer parameters for modern broadcasting standards with long time interleaving (e.g. for physical layer interleaver size, link layer protection time). Therefore, different concepts improving the state duration modelling were introduced: semi-Markov chains [10] and dynamic Markov chains [9]. For these approaches some exemplary parameters for the single-satellite reception are published. However, an intense study for multi-satellite state duration modelling and a corresponding channel model including parameters for different environments and orbital positions does not exist so far. In this sense, a new channel model for two or more satellites was developed in the context of the project MiLADY (*M*obile satell*i*te channe*L* with *A*ngle *D*iversit*Y*) [11]. This project covered two measurement campaigns in the U.S. and in Europe: In the first campaign the power levels of the Satellite Digital Audio Radio Services (SDARS) satellites (S-Band) were recorded synchronously with a sample rate of 2.1 kHz. The signals allow to study slow and fast fading effects in combination with angle diversity for a limited set of elevation and azimuth angle combinations. A second measurement campaign was carried out in the area of Erlangen in Germany to record the carrier-to-noise spectral density ratio (C/N_0) from Global Navigation Satellite System (GNSS) satellites in the L-Band. The C/N_0 allows a comprehensive analysis of the state correlation (line of sight, shadowed/blocked) for multiple satellites for a wide range of elevation and azimuth angle combinations.

This article focuses on the state sequence generation for a dual-satellite channel model. The parameters are derived from the measurements for different modelling approaches assuming two states per satellite ('good', 'bad'). Chosen models are: first-order Markov approach [7], semi-Markov approach [10], and dynamic Markov approach [9]. To assess the performance of these models, correlation coefficients, state probabilities and state duration statistics are gained from re-simulated state sequences and compared with the measurement data. As state sequence modelling is only a part of a complete LMS channel model, we describe an overall LMS channel model and give the complete set of parameters.

The article is organised as follows: In Section 2 basics of the LMS channel and of different state modelling methods for single- and dual-satellite reception are explained. Further on, these methods are compared on an exemplary scenario for two satellites. Section 3 gives an overview on the GNSS and SDARS measurements and the data processing to derive the channel states. In Section 4 the state models are compared on a high number of receive scenarios with the measurements. The evaluation criteria are state probabilities and state duration statistics. Finally, in Section 5 the conclusions are drawn.

2 Statistical channel modelling for single-satellite and dual-satellite systems

The statistical approach of generating time series for the LMS propagation channel includes two processes: First, the very slow fading components of the channel due to varying shadowing conditions between the satellite and the receiver are modelled in terms of channel states. LMS models with three states [3], namely 'line-of-sight', 'shadowed', and 'blocked', or two states [2,4] 'good' and 'bad' are available in the literature. Once the channel states are modelled, in a second process the amplitudes of direct and indirect signal components are generated. They depend on the current state and the receive environment. In common narrowband LMS propagation models the fading is described as a combination of log-normal, Rice and Rayleigh models.

In Figure 1 the two-state approach according to Prieto-Cerdeira et al. [4] is illustrated. This model describes two states: a 'good' state (corresponding to LOS/light shadowing), and a 'bad' state (corresponding to heavy shadowing/blockage). Within each state a Loo-distributed fading signal [1] is assumed. It includes a slow fading component (lognormal fading) corresponding to varying shadowing conditions of the direct signal, and a fast fading component due to multipath effects. The Loo model is described by three parameters M_A, Σ_A, and MP, denoting the mean and standard deviation of the lognormal component, and the multipath power, respectively. After each state transition a random Loo parameter triplet is generated following a statistical distribution. The distribution of the Loo parameter triplets depends on the current state, and further on the receive environment of the terminal. This two-state model is an evolution of an earlier three-state model [3], where the Loo parameter triplet for each state was fixed within a given environment and elevation. The versatile Loo parameter selection of the newer model enables a more realistic modelling over the full

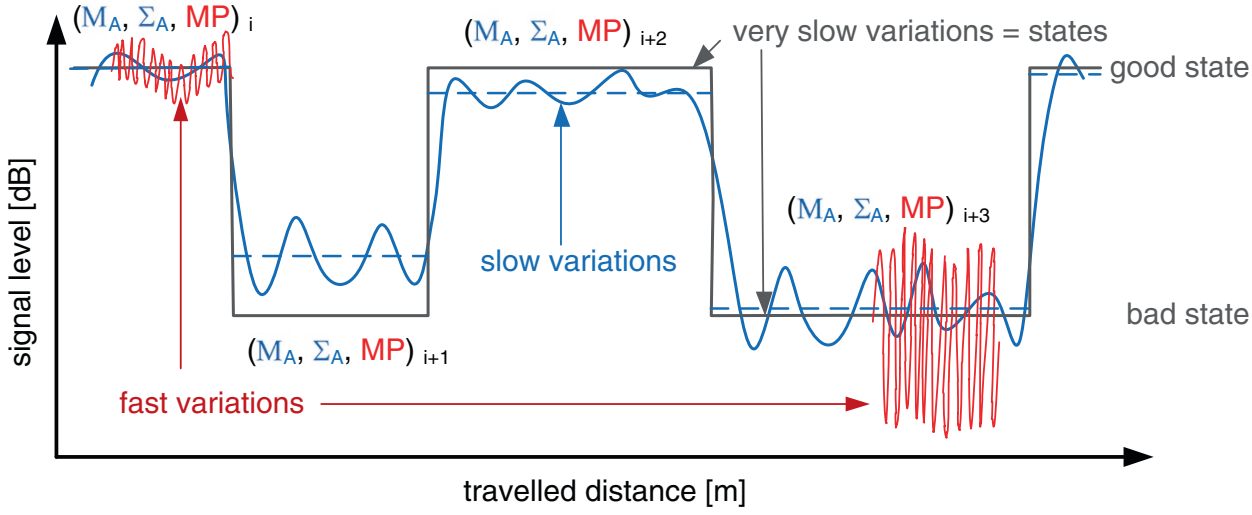

Figure 1 Signal components of a two-state LMS channel model.

dynamic range of the received signal. Therefore, the two-state model from Prieto-Cerdeira et al. [4] was extended for the new multi-satellite narrowband model developed within the MiLADY project.

Focus of this article is the state sequence modelling for single- and dual-satellite systems, assuming two states per satellite: 'good' state and 'bad' state. For this purpose, different state modelling methods are compared with the measurement data in terms of the state probability, state duration probability, and correlation coefficient. Moreover the practicability of various state generation methods in terms of generating a database, e.g. for different environments and elevation angles, is assessed.

2.1 Channel state models for single-satellite systems

Three types of state modelling approaches for single-satellite systems are found in the literature:

- First-order Markov model [3]
- Dynamic Markov model [9]
- Semi-Markov model [10]

In the following the main characteristics of these models are described.

2.1.1 First-order Markov model

A Markov model is a special random process for generating discrete samples corresponding to channel states s of a predefined sample length. For a first-order Markov model, each state depends only on the previous state. The conditional probabilities of state s_{n+1} given the state s_n are described by state transition probabilities p_{ij}. Therefore, the only parameter of the Markov chain is the state transition probability matrix (STPM) $\mathbf{P}_{\text{trans}} \in \mathbb{R}_{0+}^{N\times N}$ with N being the number of states (cf. Figure 2a). The main characteristic of a first-order Markov chain is, that it enables an exact modelling of the state probability and the average state duration. It satisfies

$$\mathbf{p}\cdot[\,\mathbf{P}_{\text{trans}} - \mathbf{I}] = \mathbf{0} \tag{1}$$

with $\mathbf{p}$ being the row vector of the equilibrium state probabilities, the unity matrix $\mathbf{I}$, and the zero vector $\mathbf{0}$.

The average state duration is calculated by

$$\bar{D} = \frac{1}{1-p_{ii}} \cdot \frac{1}{\Delta d}, \tag{2}$$

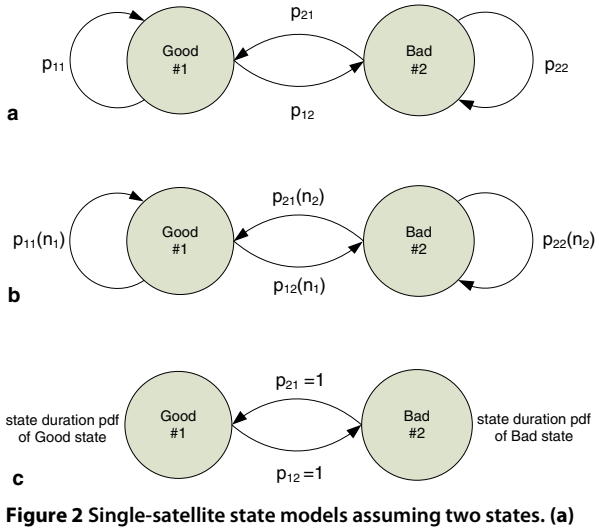

Figure 2 Single-satellite state models assuming two states. **(a)** First-order Markov model. **(b)** Dynamic Markov model. **(c)** Semi-Markov model.

where p_{ii} is the state transition probability between two equal states, and Δd denotes the sampling distance (frame length).

The probability that the Markov chain stays in state i for n consecutive samples is given by

$$P_i(D = n\Delta d) = p_{ii}^{n-1} \cdot (1 - p_{ii}), \quad n \in \mathbb{N}, \tag{3}$$

In this article the function $P(D)$ will be further denoted as state duration probability density function (SDPDF). The SDPDF of the first-order Markov chain follows an exponential distribution.

2.1.2 Dynamic Markov model

Results in [9,10] have shown that an exponential SDPDF is no accurate approximation for the LMS channel. Therefore, to improve the state duration modelling dynamic Markov chains were introduced [9]. For dynamic Markov chains the state transition probability is a function of the current state duration n (cf. Figure 2b)

$$p_{ij} = f(n). \tag{4}$$

For this purpose, the two-dimensional STPM is extended to a three-dimensional state transition probability tensor (STPT) $\mathcal{P}_{\text{trans}} \in \mathbb{R}_{0+}^{N \times N \times n_{\max}}$, where $n_{\max}$ corresponds to the maximum state length obtained from the measurements with $D_{\max} = n_{\max}\Delta d$.

Using the dynamic Markov model, the probability that the state duration is equal to D is

$$P_i(D = n\Delta d) = (1 - p_{ii}(n\Delta d)) \cdot \prod_{r=1}^{n-1} p_{ii}(r\Delta d), \quad n \in \mathbb{N}. \tag{5}$$

If the values for the STPT are directly derived from the measured state sequence (assuming a sample length of e.g. $\Delta d = 1$m), the dynamic Markov model enables an exact reproduction of the state probabilities as well as an exact re-modelling of the measured SDPDF. A significant disadvantage is the high number of parameters required to describe the STPT.

In [9] some model approximations are proposed to reduce the number of required parameters of the STPT:

- partial dynamic Markov model: From Equation (5) it is derived that an exact state duration modelling requires only a subset of the STPT. Only the transition coefficients $p_{ii}(n)$ need to change as a function of the current state duration. For a two-state model the remaining values $p_{ij}(n)$ can be recalculated easily with $p_{ij}(n) + p_{ii}(n) = 1$. For a multi-state model some additional coefficients S_{iZ} are required to calculate the relative ratio between the state transition probabilities $p_{ij}(n)$. The coefficients are derived from the STPT $\mathcal{P}_{\text{trans}}$ at position $n = 1$ for each state i

$$p_{ii}(1) + S_{i1}(1) + S_{i2}(1) + \cdots + S_{iZ}(1) = 1, \quad \text{with } S_{iZ}(1) = p_{ij}(1), i \neq j. \tag{6}$$

  Then, to calculate the relative coefficients at positions $p_{ij}(n > 1)$ it holds:

$$p_{ii}(n) + kS_{i1} + kS_{i2} + \cdots + kS_{iZ} = 1, \quad \text{with } kS_{iZ} = p_{ij}(n). \tag{7}$$

- approximated partial dynamic Markov model: For a further reduction of the model parameters, the function $p_{ii}(n)$ can be approximated by a curve fit. In [9], a piecewise linear approximation at 8 predefined values of the state duration $D = n\Delta d$ is proposed. Assuming this, a two-state model would require $8 \cdot 2$ parameters for state sequence generation. A multi-state model would need $8 \cdot N$ parameters to describe the functions $p_{ii}(n)$ (with N being the number of states) and further $N(N-1)$ parameters to describe the relative ratios S_{iZ} between the coefficients $p_{ij}(n), i \neq j$ (Equation (6)).

2.1.3 Semi-Markov model

Another Markov approach is the semi-Markov model introduced in [10] to enable a correct state duration modelling. In contrast to the first-order- and dynamic Markov model, the state transitions do not occur at concrete time intervals. In fact, the time interval of the model staying in state i depends directly on its SDPDF. As with the Markov models, the state transitions are described with the state transition probability p_{ij}, but with $i \neq j$. Assuming a single-satellite model of only two states, the state transition probability is $p_{ij} = 1$ (cf. Figure 2c). The equilibrium probability of the states can be calculated as the product of the mean state duration $\bar{D}$ and the probability of entering a state (which is described with the STPM).

The semi-Markov model offers some options to describe the SDPDF of each state:

- The measured state duration statistic is used without any approximation for re-modelling, i.e., the state duration is a random realisation of the measured SDPDF.

$$P(D) = P(D_{\text{measured}}) \tag{8}$$

- The measured SDPDF is approximated with a log-normal distribution, as proposed in [4,10] individually for the single-satellite state 'good' and 'bad'. The lognormal probability density function describing the state duration probability $P(D)$ is given by

$$P(D) = \frac{1}{D\sigma\sqrt{2\pi}} \exp\left[-\frac{(\ln(D) - \mu)^2}{2\sigma^2}\right], \tag{9}$$

  where σ is the standard deviation of $\ln(D)$ and μ is the mean value of $\ln(D)$. Using this approximation, only two parameters per state are required to

describe the SDPDF. The mean state duration $\bar{D}$ can be calculated with

$$\bar{D} = \exp\left[\mu + 0.5\sigma^2\right]. \tag{10}$$

- In [9], a piecewise exponential curve fit of the SDPDF using four segments is proposed. Clearly, this requires more parameters than the lognormal curve fit, but it enables a more flexible re-modelling of the state duration statistic.

$$P(D) = \begin{cases} a_1\,\mathrm{e}^{-b_1 D}, & D_0 \le D \le D_1 \\ a_2\,\mathrm{e}^{-b_2 D}, & D_1 \le D \le D_2 \\ a_3\,\mathrm{e}^{-b_3 D}, & D_2 \le D \le D_3 \\ a_4\,\mathrm{e}^{-b_4 D}, & D_3 \le D \le D_4 \end{cases} \tag{11}$$

In any case, the STPM has to be derived from measurements, which is independent from the used SDPDF approximation.

State probability and mean state durations of semi-Markov chains: In some cases, an approximation of the state duration with a lognormal distribution or a piecewise curve fit changes the mean state length and consequently the total probability of the states. To enable an exact description of $\bar{D}$ and P anyway, a correction of the curve fit can be implemented. For example: for the lognormal fit the parameter μ can be modified with

$$\mu_{\text{corrected}} = \ln\left[\frac{\bar{D}_{\text{measured}}}{\exp(0.5\sigma^2)}\right]. \tag{12}$$

2.2 Channel state models for dual-satellite systems

2.2.1 Straightforward method

All of the state modelling methods for the single-satellite reception mentioned in the previous section can be easily adapted for dual-satellite modelling. This can be done by combining the single-satellite states 'good' and 'bad' from two satellites to four joint states: 'good good', 'good bad', 'bad good', 'bad bad'. Therefore, Figure 3 exemplarily shows the semi-Markov model for two satellites. In case of the first-order Markov model, the 2×2 STPM becomes a 4×4 STPM. For the dynamic Markov model a $4 \times 4 \times n_{\max}$ STPT is required for the state series simulation. In case of the semi-Markov approach a 4×4 STPM and four separate state duration statistics are required for the dual-satellite modelling (Figure 3). Once the joint state sequence of four states is generated, it finally can be decomposed to extract two separate single-satellite state sequences.

2.2.2 Approximation of joint state duration statistics for semi-Markov chains

The lognormal distribution is accepted for single-satellite state duration modelling in the literature [4,10]. In the sequel, we use it for the dual-satellite case, too. To illustrate some limitations, we discuss two border cases:

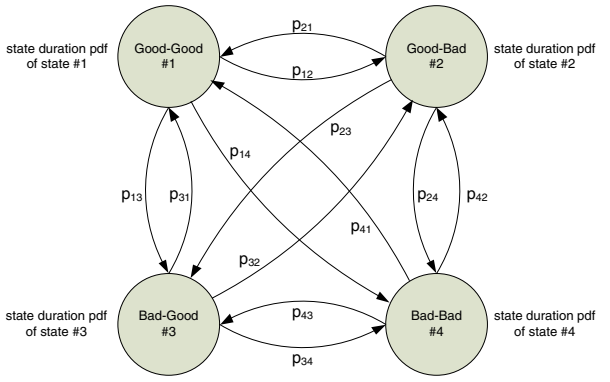

Figure 3 Semi-Markov model for two satellites.

Example 1: Two satellites are modelled independently. Figure 4 (left) shows an *ideal* lognormal distribution of the 'good' state of satellites 1 and 2 and the expected distribution of the combined state 'good good'.

Example 2: Assuming two satellites having the same elevation and a marginal azimuth separation. The state sequence from satellite 2 is exactly the same as the state sequence from satellite 1, but with a delay of 5 m. As a result, the state duration distribution for 'good bad' or 'bad good' is limited to the range of [0 m; 5 m] and has a peak at 5 m (cf. Figure 4 (right)).

Both examples show that a curve-fit of the joint state duration requires some degree of flexibility. A good fit would be a piecewise approximation. Nevertheless, when analysing real measurement data it is obtained that already a (simple) lognormal fit provides good approximations of the state durations, as shown later in this article.

2.2.3 Lutz model

Besides the above straightforward method of extending multiple single-satellite states to joint states, a very effective approach for two correlated satellites was introduced in [7]. This algorithm is based on first-order Markov chains and generates a joint STPM (4×4 elements) from two independent single-satellite STPMs (each with 2×2 elements). Using the joint STPM, a joint sequence of four states can be generated as mentioned above. The high flexibility of this algorithm becomes clear, since it requires only single-satellite parameter sets (in form of 2×2 STPMs), that are easy to parametrise and are already available in literature for different elevation angles and a high number of environments. Databases for correlation coefficients are available for different environments, elevation angles, and angular separations of the azimuth and elevation angle [6] as well.

In contrast to this Lutz model, the above mentioned 'straightforward methods' need complete datasets for any

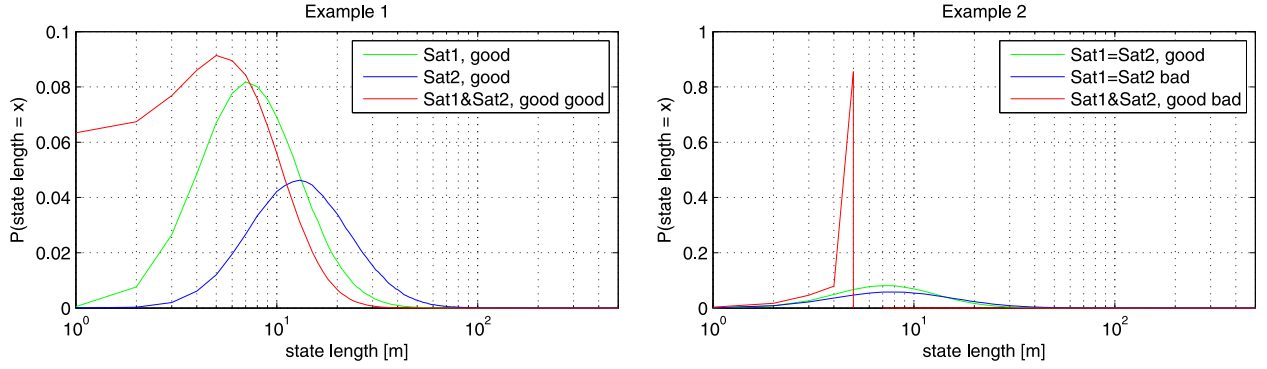

Figure 4 Preliminary consideration for joint state distributions. Two examples for the expected distribution of the joint states with the assumption, that the single satellite states are lognormal distributed.

combination of elevation angles, azimuth angle separations and environments to achieve the same variability.

2.3 Comparison of state models for dual-satellite systems

In this section different state modelling methods for dual-satellite reception are compared based on an exemplary scenario extracted from the GNSS measurements (we chose: urban environment, elevation1 $= 45°$, elevation2 $= 25°$, azimuth angle separation$= 45°$). Six different approaches are applied to re-simulate this scenario. For this purpose, Table 1 shows the joint state probabilities $P_{\text{jointState}}$, the single-satellite state probabilities P_{state}, the correlation coefficient ϱ_{states}, and the number of parameters required for the models. Further on, in Figure 5 the state duration statistics are presented for the joint states and the single-satellite states derived from the measurements and after simulation with different algorithms. The quality of the state duration modelling from Figure 5 is analysed in terms of the mean squared error (MSE) between measured and re-simulated state duration PDF (cf. Table 2).

From Figure 5, Table 1, and Table 2 the following results are obtained:

- first-order Markov model (Lutz model)
  - perfect match of P_{state} and ϱ_{states} according to theory, furthermore $P_{\text{jointState}}$ is estimated correctly
  - some deviations between the state duration statistics and the measurements. The MSE of the SDPDF is high compared to other algorithms.
- dynamic Markov model
  - perfect match of $P_{\text{jointState}}$, P_{state}, and ϱ_{states}
  - according to theory, joint state durations are modelled accurate (MSE $= 0$)
  - good (but not perfect) match of the single-satellite state durations

Table 1 Measured and re-simulated state probabilities and state correlation coefficients using different dual-satellite state models for an exemplary scenario: urban, elevation1 $= 45°$, elevation2 $= 25°$, azimuth separation $= 45°$ (g. . . 'good'-state, b. . . 'bad'-state, gb . . . 'good bad'-state, etc.)

Algorithm	Corr.	Joint state prob. (Sat1 & Sat2)				Sat1		Sat2		Parameters
	coef.	P_{gg}	P_{gb}	P_{bg}	P_{bb}	P_{g}	P_{b}	P_{g}	P_{b}	
measured (Reference)	**0.15**	**0.32**	**0.46**	**0.05**	**0.16**	**0.78**	**0.22**	**0.37**	**0.63**	
1st order Markov (Lutz)	0.15	0.32	0.46	0.05	0.16	0.78	0.22	0.37	0.63	9
dynamic Markov	0.15	0.32	0.46	0.05	0.16	0.78	0.22	0.37	0.63	11120
partial dynamic Markov	0.10	0.35	0.37	0.10	0.17	0.72	0.28	0.45	0.55	2792
Semi-Markov, no fit	0.15	0.32	0.46	0.05	0.16	0.78	0.22	0.37	0.63	2796
Semi-Markov, lognormal fit	0.15	0.33	0.46	0.05	0.16	0.79	0.21	0.38	0.62	20
Semi-M., logn.fit + correction	0.15	0.32	0.46	0.05	0.16	0.78	0.22	0.37	0.63	20
Semi-Markov, piecew. exp. fit	0.15	0.33	0.45	0.05	0.17	0.78	0.22	0.38	0.62	64

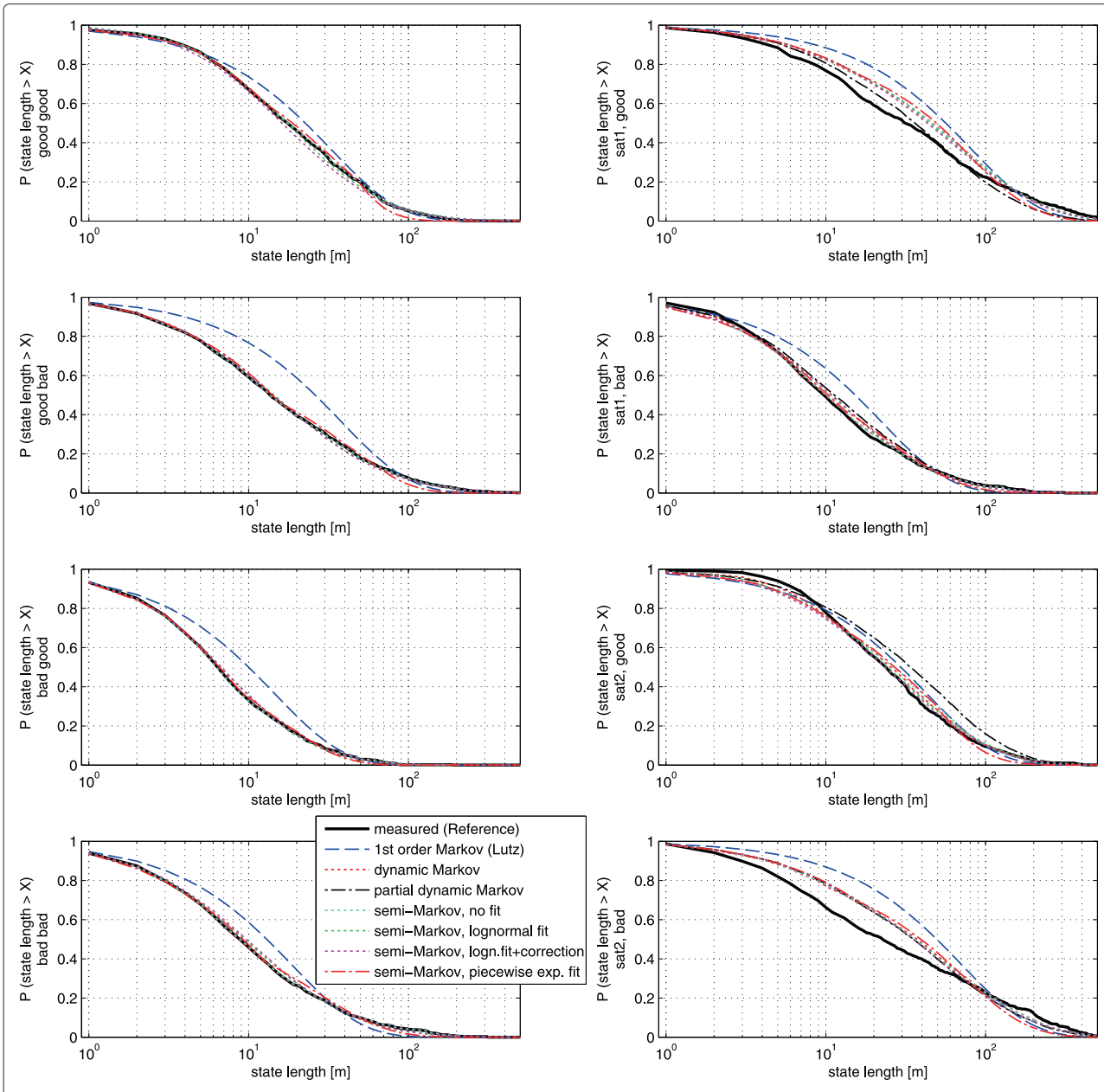

Figure 5 State duration statistics for different state models. Measured and resimulated state duration statistics of two single satellites (right) and of the combined states (left) for a single scenario (urban, elevation1 = 45°, elevation2 = 25°, azimuth separation = 45°). Each model generates a combined state sequence of 'good good', 'good bad', 'bad good', and 'bad bad'. To get the state sequences of the individual satellites this joint sequence is decomposed afterwards. The ideal dual-satellite model should describe correctly the state duration statistics and the state probabilities of the joint states as well as the state duration statistics and the state probabilities of each single satellite.

- partial dynamic Markov model
  - perfect match of joint state durations (MSE = 0)
  - good match of the single-satellite state durations
  - despite the high model complexity, $P_{\text{jointState}}$ and P_{state} can not be re-modelled accurately
- semi-Markov with measured SDPDF
  - perfect match of $P_{\text{jointState}}$, P_{state}, ϱ_{states}, and joint state duration statistics
  - good match of single-satellite duration statistics
  - same results as with the dynamic Markov model, but with less parameters

Table 2 Mean Squared Error (MSE) of the re-simulated state duration PDF to the measured state duration PDF using different dual-satellite state models for an exemplary scenario (cf. Figure 5)

Algorithm	MSE in $[10^{-5}]$ for Sat1 & Sat2				MSE in $[10^{-5}]$ for Sat1		MSE in $[10^{-5}]$ for Sat2		Parameters
	gg	gb	bg	bb	g	b	g	b	
1st order Markov (Lutz)	0.41	0.99	1.19	0.72	0.72	1.10	0.67	1.36	9
Dynamic Markov	0	0	0	0	0.31	0.15	0.23	0.47	11120
Partial dynamic Markov	0	0	0	0	0.28	0.28	0.53	0.57	2792
Semi-Markov, no fit	0	0	0	0	0.33	0.25	0.34	0.58	2796
Semi-Markov, lognormal fit	0.23	0.17	0.19	0.13	0.39	0.38	0.45	0.67	20
Semi-Markov, logn.fit + correction	0.24	0.17	0.21	0.17	0.40	0.36	0.47	0.67	20
Semi-Markov, piecewise exp. fit	0.24	0.19	0.21	0.23	0.42	0.45	0.54	0.64	64

- semi-Markov with lognormal-fit
  - marginal differences of $P_{\text{jointState}}$, P_{state}, and ϱ_{states} from measurements
  - good match of the of joint states and single-satellite state durations: the MSE is much lower compared to first-order Markov models, but higher than dynamic Markov models
- semi-Markov with lognormal-fit and correction of mean state duration (cf. Equation (12))
  - due to the modification, perfect match of $P_{\text{jointState}}$, P_{state}, and ϱ_{states}
  - since the correction of the state duration is only marginal, the MSE is marginal greater than the initial lognormal-fit
- semi-Markov with piecewise exponential approximated SDPDF
  - marginal differences of $P_{\text{jointState}}$, P_{state}, and ϱ_{states} from measurements
  - good match of duration statistics for joint states and single-satellite states

Based on the previous results, Table 3 presents a comparison of the channel models in terms of complexity, their accuracy for state probability modelling, and their capability for state duration modelling.

With respect to the required number of parameters, it can be concluded that the 'dynamic Markov model' (no approximations) and the 'semi-Markov model with measured SDPDF' are not feasible to generate a dual-satellite model database representing arbitrary receive situations, although they achieve a perfect re-modelling of state probabilities and state duration statistics. The 'partial dynamic Markov model' (and consequently its approximated versions) is not able to reproduce the state probabilities correctly. As a consequence, its applicability for state modelling is limited. The Lutz model, the semi-Markov model with a lognormal SDPDF, and the semi-Markov model with a piecewise exponential approximated SDPDF achieve good modelling results by using an acceptable number of parameters. These three models are compared in Section 4 using a large number of receive scenarios.

2.4 Channel state models for multi-satellite systems

In general, all state models mentioned in the previous subsections are extendable to multiple satellites. However, the number of required parameters for the models grows exponentially with the number of satellites. To avoid excessive complexity for the state modelling with more than two satellites, a 'Master–Slave' approach is planned [11]. Within the Master–Slave approach it is assumed that each 'Slave' satellite depends only on a 'Master' satellite, whereas the correlation between the slaves is not described (cf. Figure 6).

Table 3 Performance comparison of dual-satellite state models

Algorithm	State probability modelling	State duration modelling	Model complexity
1st order Markov (Lutz)	perfect	bad	low
Dynamic Markov	perfect	perfect	high
Partial dynamic Markov	bad	perfect	high
Semi-Markov, no fit	perfect	perfect	high
Semi-Markov, lognormal fit	good	good	medium
Semi-Markov, logn.fit+correction	perfect	good	medium
Semi-Markov, piecewise exp. fit	good	good	medium

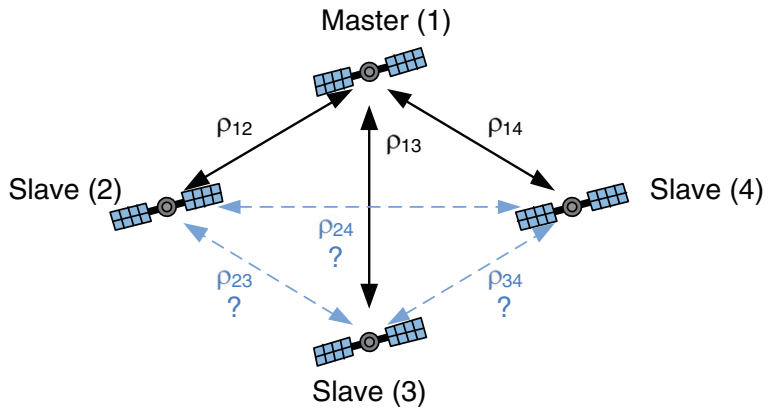

Figure 6 Master–Slave approach for multi-satellite modelling. Several 'Slave' satellites are modelled according to the correlation to one 'Master' satellite, while neglecting the correlation between the 'Slave' satellites. The Master–Slave method has a reduced complexity compared to the conventional approach, where each individual correlation is described.

Some preliminary investigations of this concept for dual-satellite reception yields that correlation coefficients, state probabilities of single satellites, and joint state probabilities can be modelled accurately, whereas a correct state duration modelling of the Slaves has limitations.

To validate the Master–Slave concept for multi-satellite reception, a statistical analysis for constellations with at least three satellites needs to be performed. This is addressed in near future activities.

2.5 Dual-satellite LMS model with correlated state sequences

In the context of the project MiLADY, extensive satellite signal measurements were analysed to develop a new multi-satellite channel model. The basis is the two-state model from Prieto-Cerdeira et al. [4]. It includes a versatile selection of Loo-parameter triplets after each state transition to describe slow and fast signal variations.

However, the analysis of the measurement data captured in the MiLADY project indicate some changes to the initial two-state model [4] in terms of describing slow and fast fading characteristics. Further on, correlation effects for slow and fast variations between the satellites were obtained from the data. A comprehensive study for slow and fast fading effects is topic of ongoing work and out of scope of this article.

For a preliminary simulation of timeseries for dual-satellite reception, Figure 7 shows the structure of a dual-satellite channel model with correlated state sequences. It was found, that correlated state sequences dominates the satellite signals correlation. They are jointly modelled in the state sequence generator (SSG). For the simulation of slow and fast variations, we also derived Loo parameters from the SDARS measurements. They are to be applied

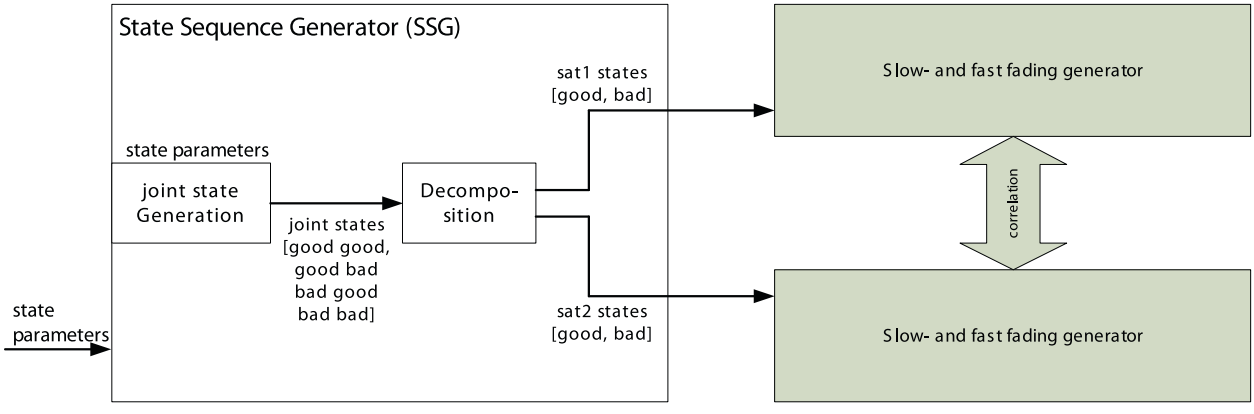

Figure 7 Building blocks of the dual-satellite channel model with correlated state sequences. Slow and fast fading can be preliminary generated according to Prieto-Cerdeira et al. [4] without regarding a correlation between the satellites. A comprehensive study about the correlation of small-scale signal variations as well as a modification of the 'Slow and fast fading generator' is out of scope of this article.

according to Prieto-Cerdeira et al. [4] and can be found in the Additional file 1.

3 Satellite signal measurements and data processing for angle diversity analysis

To derive the parameters for a new multi-satellite LMS model, two measurement campaigns were carried out in the context of the MiLADY project.

3.1 SDARS measurements, U.S. east coast

In a first campaign the power levels of the SDARS satellites (S-Band) were recorded along the east coast of the U.S. (cf. Figure 8). The signals were sampled with 2.1 kHz, that allows to derive all dual-satellite model parameters for very slow variations (state parameters) and slow- and fast variations (Loo parameters). However, based on two geostationary satellites and two satellites in the high elliptical orbit only a few orbital constellations can be gained. The US campaign and measurement statistics were described in detail in [11,12].

3.2 GNSS measurements, Erlangen, Germany

A second measurement campaign was carried out around Erlangen (Germany) to record the carrier-to-noise spectral density ratio (C/N_0) from GNSS satellites in the L-Band. Due to a permanent availability of at least eight satellites on the hemisphere, a comprehensive analysis of fading effects for a wide range of elevation and azimuth angle combinations of multiple satellites is possible. Because of the low C/N_0 resolution in time (20 Hz) and in amplitude (1 dB quantisation), only parameters for slow variations can be derived.

The GNSS campaign was split in two parts:

- The first part of the campaign has been carried out in July 2009. The GNSS antenna was mounted on a measurement van at a height of 2 m. A measurement round-trip of 38 km length was driven ten times, covering several environments (suburban, forest, open, commercial) in and around Erlangen (cf. Figure 8, red line).
- The second part of the measurements was done in late September and early October 2010 by mounting the setup onto two city buses, driving on different routes. The GNSS antenna was mounted at a height of 3.1 m. The city buses drove an identical route for 3 days. The covered environments were urban, suburban and partly open rural areas. The individual routes of the two buses spanned 7 km and 6 km in North–South direction and 6 km and 5 km in West–East direction, respectively (cf. Figure 8, green and yellow line).

The trials were carried out in summer and in autumn months, where leaves were on the trees.

For the measurements a professional GNSS receiver (built by Fraunhofer IIS by using a Javad receiver core) was used. Beside information of vehicle speed and positioning data, the GNSS signal includes a C/N_0 estimation of the GPS L1 carrier at 1575.420 MHz. It has a dynamic range of 20 dB and a quantisation of 1 dB. The time resolution of the C/N_0 estimation is 20 Hz. At lower signal levels of a specific satellite (e.g. during deep blockages), the GNSS receiver loses the satellites signal synchronisation and the C/N_0 estimation of this satellite is no more available. In terms of state detection it will be defined as 'bad' state. Additional information of azimuth and elevation of the individual satellites were captured with 1° resolution.

Table 4 summarises the main aspects of the two MiLADY measurement campaigns.

3.3 Data processing and state identification

The analysis pipeline for both the SDARS and GNSS data is similar. First, the signal is normalised to LOS level [13].

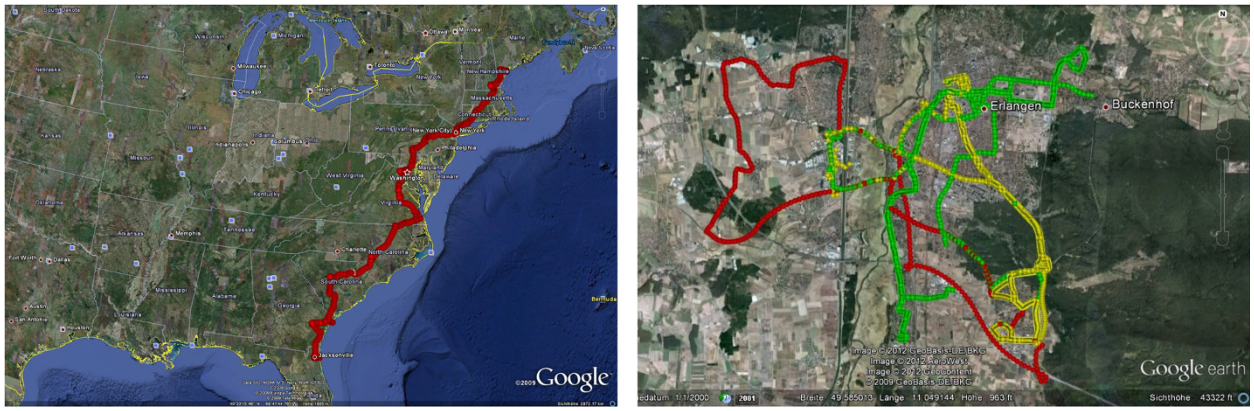

Figure 8 Measurement campaigns within the project MiLADY. Left: SDARS measurements along the U.S. East Coast. Right: GNSS measurements in area of Erlangen, Germany. The colors indicate three parts of the GNSS measurements with a van (red), and two city buses (green and yellow).

Table 4 Overview on two measurement campaigns for the parameter extraction of a multi-satellite LMS model

SDARS measurements (USA, East Coast)	GNSS measurements (Germany, Erlangen)
High sample rate (2.1 kHz)	Low sample rate (20 Hz)
→ Reliable for Loo parameter extraction and state parameter extraction	→ Reliable for state parameter extraction
4 satellites (2 GEO from XM, 3 HEO from Sirius)	>20 satellites (MEO from GPS, GLONASS)
→ Limited combinations of orbital positions	→ Many combinations of orbital positions
Environments: urban, suburban, tree-shadowed, forest, commercial, highway (open)	Environments: urban, suburban, forest, commercial, open
Model validation for a limited set of orbital positions	Preliminary state parameters for many orbital positions which need refinement and validation

Afterwards, the timeseries is re-sampled into travelled distance units. As resolution, 1 cm and 10 cm is chosen for the SDARS and GNSS data, respectively. State identification is performed by global thresholding (threshold 5 dB below LOS) of the low-pass filtered signal (sliding window over 5 m), similar to [10].

Figure 9 shows example measurement sequences from GNSS and SDARS trials, which are separated into two states.

3.4 Separation of data into environments and satellite positions

3.4.1 Single-satellite analysis

Single-satellite reception depends on the kind of environment, the elevation angle of the satellite, and the azimuth of the satellite relative to the driving direction. For a detailed analysis of the single-satellite state characteristics, the SDARS- and GNSS measurement data were divided into:

- different environment types 'Urban', 'Suburban', 'Forest', 'Commercial', and 'Open'. The environment classification for the SDARS measurement data was performed by visual inspection of the image material from two cameras. For the GNSS measurement data the Land-Usage data from the European Corine project [14] was used.
- different elevation angles from 10° to 90° in segments of 10°. The mean elevation angles represented by these datasets therefore are 15°, 25°, . . ., 85°, respectively.
- four classes of driving directions (for GNSS data, only) with the intervals 0° . . . 10°, 10° . . . 30°, 30° . . . 60°, and 60° . . . 90°.

Figure 10 shows the amount of data from SDARS and GNSS measurements for single-satellite analysis. Due to the limited amount of SDARS data (except highway/open environments), different driving directions are excluded from analysis.

3.4.2 Dual-satellite analysis

The dual-satellite (and multi-satellite) reception depends on the kind of environment, the elevation angle of each satellite, and the azimuth of each satellite relative to the driving direction. Especially the angular separation of the satellites of elevation and azimuth are crucial, since it affects the correlation of the received signals. For a detailed analysis of state characteristics for dual-satellite reception, the measurement data from SDARS and GNSS measurements were divided into:

- five environments (the same as for single-satellite case).
- combinations of eight elevation angles as used for single-satellite analysis. Thus, the elevation angle separation is included as well.

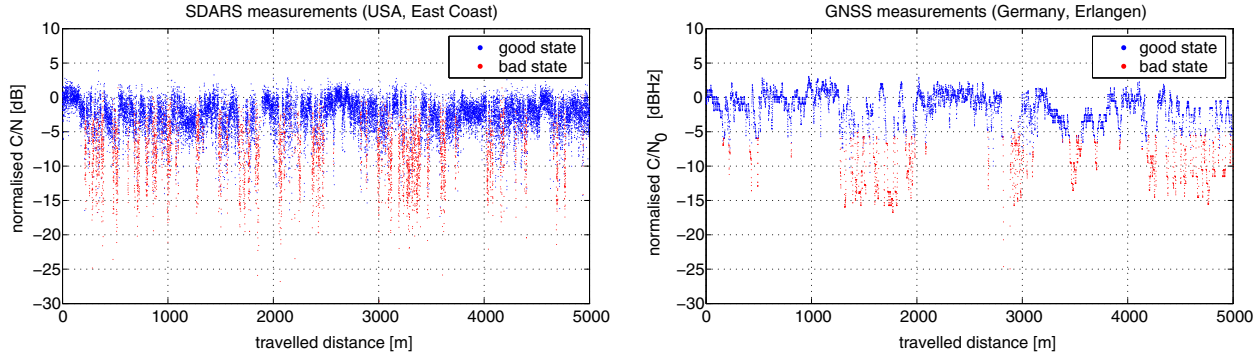

Figure 9 Exemplary measurement signals from two campaigns separated into 'good' state and 'bad' state. Left: normalised C/N from SDARS measurements in the USA. Right: normalised C/N_0 estimation at the GNSS receiver from measurements in Germany.

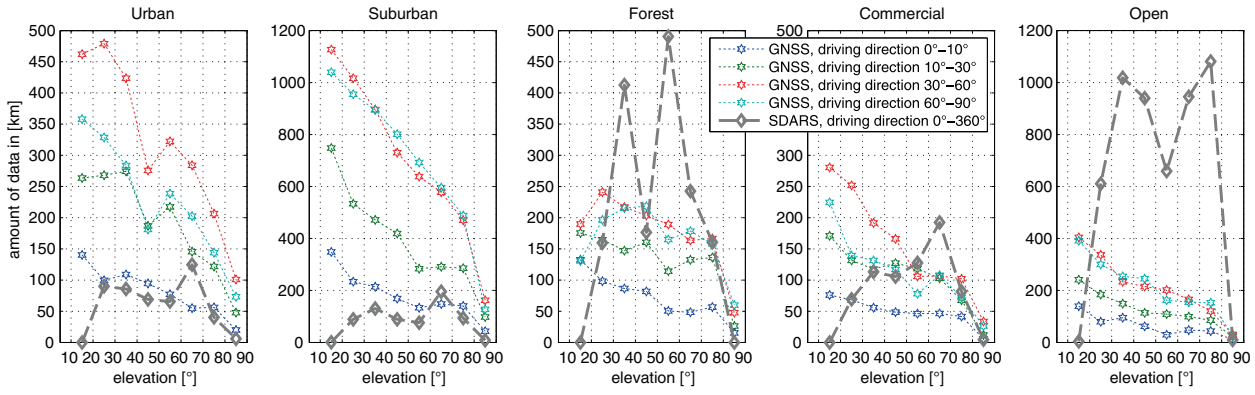

Figure 10 Amount of data for single-satellite reception. Amount of data from SDARS measurements and GNSS measurements for different environments and elevation angles. Please note that the values are only connected for better visibility.

- seven intervals of the azimuth angle separation between the satellites (0° . . . 10°, 10° . . . 30°, 30° . . . 60°, 60° . . . 90°, 90° . . . 120°, 0° . . . 150°, and 150° . . . 180°).

This adds up to a total of $5 \cdot 8 \cdot 8 \cdot 7 = 2,240$ segments (further denoted as *receive scenario*) of measurement data. A further division into driving directions was omitted. For a reliable dual-satellite state analysis (especially in terms of state duration analysis) and parametrisation of the Markov models, a minimum number of states is required. For this purpose, we define a receive scenario as 'valid' if each combined state ('good good', 'good bad', 'bad good', 'bad bad') is visited at least 50 times[a]. It corresponds to a state sequence with more than 200 state transitions. Based on this condition, Figure 11 presents the available receive scenarios for the SDARS and GNSS measurements. The dual-satellite state analysis in this article is based on the GNSS data. A dual-satellite analysis of the SDARS data is omitted, since the limited SDARS constellations restricts conclusions for dual-satellite reception in dependence on azimuth angle separation or elevation.

Figure 12 presents the amount of data within the proposed 2,240 receive scenarios sorted by measurement length, and by number of visits of the combined states. From GNSS data, about 2,000 scenarios are valid for analysis (with ≥50 visits per combined state). In the SDARS data only 200 valid receive scenarios are found. Taking the condition of ≥50 visits per combined state, the shortest measurement length is ≈4 km for GNSS and SDARS. From GNSS, about 50% of the scenarios include more than 100 km of data. Even 1% of the scenarios consists of more than 1,000 km. It allows to draw reliable statistical conclusions for dual-satellite reception. Note that the available measurement length for analysis does not directly correspond to the driven distance. It rather describes the available length after combining any of the visible satellites.

4 Measurement results and state modelling statistics

In this section the results of the GNSS and SDARS analyses are presented in terms of state probabilities and state duration statistics for different environments and orbital positions of the satellites. In two subsections the characteristics for single-satellite reception and dual-satellite reception are addressed. Furthermore, for each dual-satellite receive scenario the parameters for different channel models are derived. Thus, the re-modelling results can be compared with the measurements.

4.1 Results for the single-satellite channel

Figure 13 shows the probabilities of the 'bad'-state for single-satellite reception from SDARS and GNSS measurements for different environments and elevation angles. Since only two states are assumed, the 'good'-state probability is calculated with $P_{\text{good}} = 1 - P_{\text{bad}}$.

The following observations can be made in Figure 13:

- The 'bad'-state probability increases with increasing angle between satellite azimuth and driving direction within the interval 0° . . . 90°. Except, for high elevation angles (>70°) the influence of the driving direction is low. For system planning and the application of effective fading mitigation techniques it is important to consider the worst case (≈90° azimuth).
- In general, the 'bad'-state probability decreases with increasing satellite elevation. The slope of the curve depends on the driving direction.
- Comparing different environments, the 'bad'-state probability in urban and forest areas is on average higher than in other environments. Also the variance between the worst (90° azimuth) and best (0° azimuth) reception case is higher than in suburban, commercial and forest.

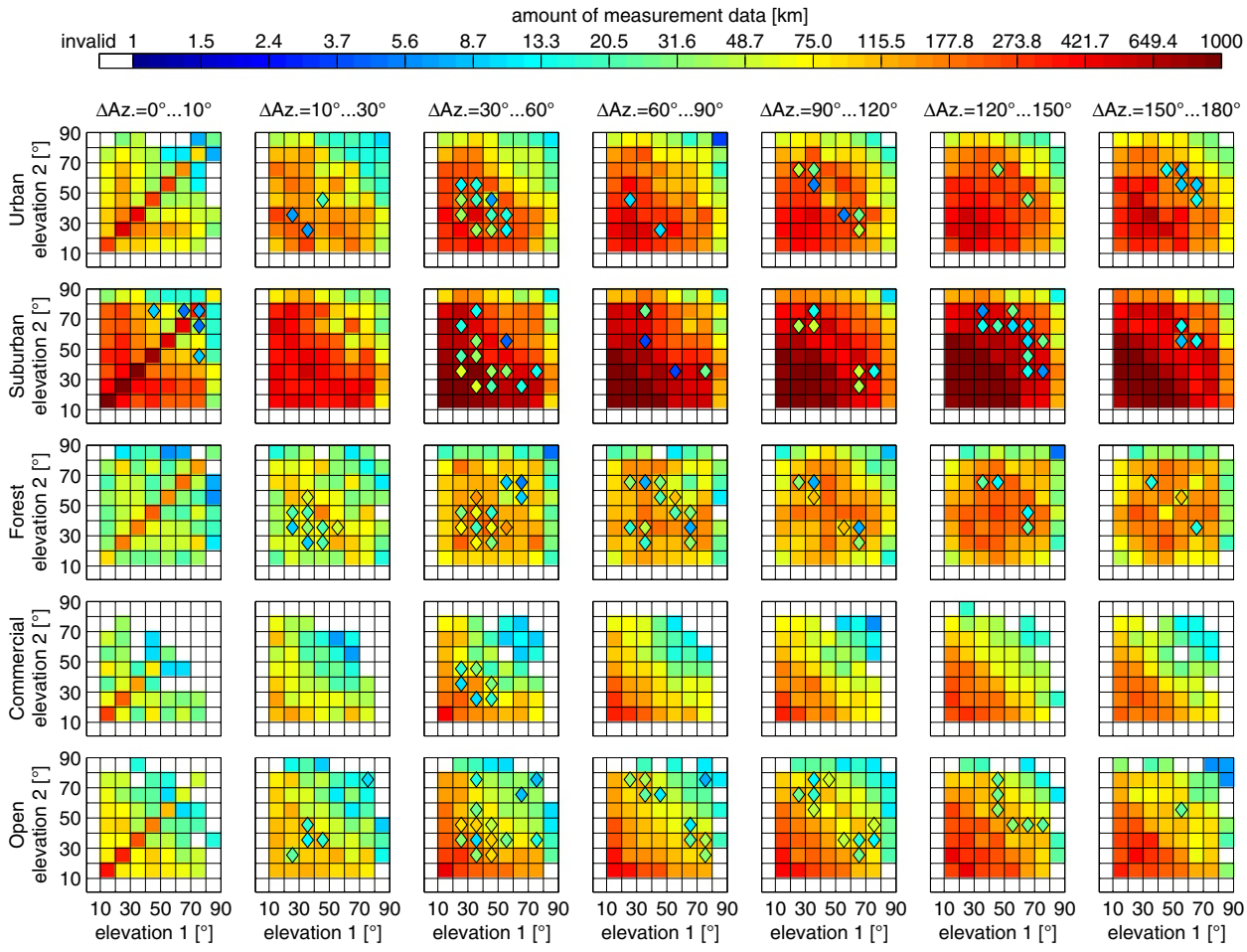

Figure 11 Available orbital constellations for dual-satellite reception. Available orbital constellations of two satellites from SDARS measurements (coloured diamonds) and from GNSS measurements (coloured fields) quantised to seven azimuth separation sections, nine elevation ranges and five environments. The colour indicates the measurement length. The GNSS data is further used for dual-satellite state analysis. A dual-satellite state analysis from SDARS is omitted, since conclusions for dual-satellite reception in dependency to azimuth angle separation or elevation are rather limited.

- In case of GNSS, for elevation angles above 70° the 'bad'-state probability in urban environments is lower than in suburban and forest environments. A reason could be that trees reach above the streets in suburban environments and forests, whereas in urban the probability of trees is low.
- Comparing SDARS and GNSS measurements similar results are obtained for urban areas only. In suburban, forest, commercial, and open environments a lower signal availability is obtained for SDARS measurements. A reason could be mainly wider streets in the U.S. than in Europe. Furthermore, for interurban measurement sections during SDARS trials the streets were mainly oriented towards the satellites. Also different methods for environment classification may have an influence to the results.

4.2 Results for the dual-satellite channel

A dual-satellite analysis was done for five different environments, the combination of eight different elevation angles from two satellites, and seven intervals of the azimuth angle separation between the satellites (cf. Figure 11). A total of $5 \cdot 8 \cdot 8 \cdot 7 = 2,240$ segments of measurement data were defined[b]. Due to that fact, displaying the results of dual-satellite modelling is much more complex than in the single-satellite case. Therefore, in this article only the urban results are presented for only a subset of receive scenarios. With regard to an acceptable number of model parameters, four state modelling approaches are selected and compared in this section: the Lutz model based on first-order Markov chains, the semi-Markov model assuming a lognormal SDPDF fit and its modification according to Equation (12), and the

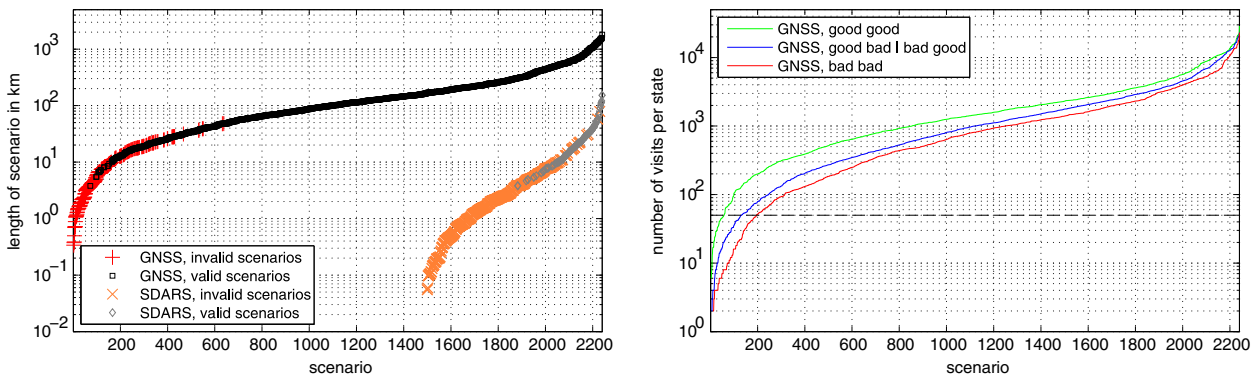

Figure 12 Amount of data for dual-satellite reception. Amount of data for dual-satellite analysis within 2,240 receive scenarios (5 environments • 8 × 8 elevation angles • 7 azimuth separations) sorted by measurement length (left) and by number of visits per combined state (right). The criterion for 'valid' scenarios is that ≥50 visits for each joint state are achieved.

semi-Markov model assuming a piecewise exponential SDPDF fit.

4.2.1 State correlation

Figure 14 shows the correlation coefficient between the states ϱ_{states} of two satellites in dependency on the azimuth separation derived from the measurements and after re-simulation with three dual-satellite state models for the urban environment. Each subplot shows a certain combination of the two elevation angles. As this matrix of subplots is symmetric, only the lower triangle is shown. For a better visibility, only the elevation angles below 50° are shown to focus on the critical receive scenarios.

The following observations can be made in Figure 14:

- In case of small azimuth separations, both state sequences are highly correlated (up to $\varrho_{\text{states}} = 0.9$). (Note: For two exactly co-located satellites $\varrho_{\text{states}} = 1$ is expected, this special case is not covered in the results.) The correlation has a minimum for azimuth separations between 60° and 120°. It can reach values $\varrho_{\text{states}} < 0$. Towards 180° azimuth separation, the correlation coefficient slightly increases.
- In case of small azimuth separation, the correlation coefficient further depends on the elevation angle separation between two satellites.
- The Lutz model perfectly re-simulates the correlation coefficient. This is not surprising, as the correlation coefficient is one parameter of the Lutz model. It combines two independent state sequences of a single-satellite simulator into a dual-satellite variant.
- A good fit of the correlation coefficients is also achieved with the semi-Markov approaches assuming a lognormal fit or a piecewise exponential fit of the

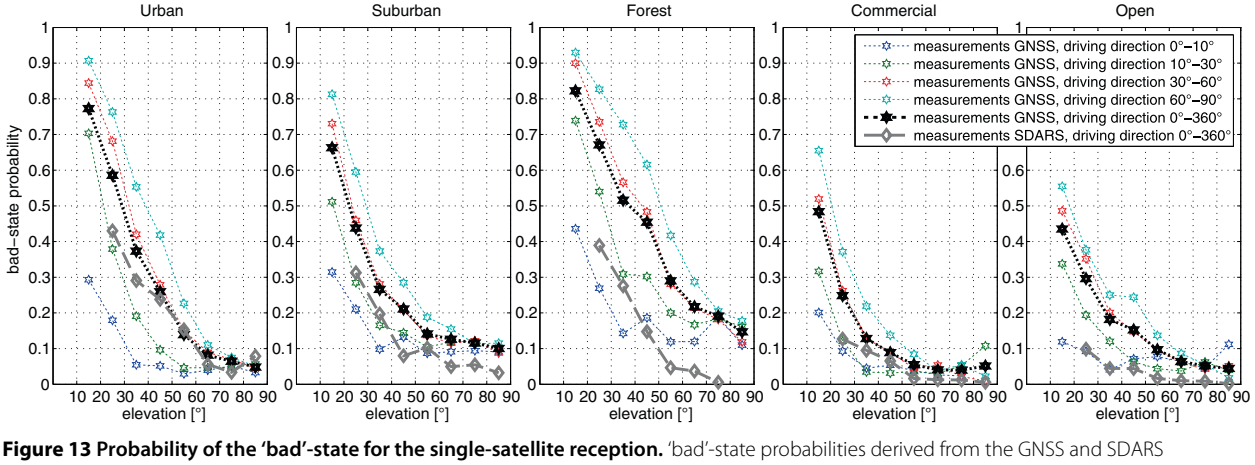

Figure 13 Probability of the 'bad'-state for the single-satellite reception. 'bad'-state probabilities derived from the GNSS and SDARS measurements for the single satellite reception in dependency to the elevation angle and the azimuth angle relative to the driving direction. The probability of the 'good' state is $1 - P_{\text{bad}}$.

SDPDF. For only a small number of receive scenarios the correlation coefficient deviates by ±0.1 from the measurements. It is acceptable, since the variation of the correlation coefficients between different elevation angles and azimuth separations is much higher.

- After a modification of the lognormal fit according to Equation (12), the correlation ϱ_{states} generated with the semi-Markov model matches exactly with the measurements.

Similar to Figure 14, the Additional files 2, 3, 4 and 5 show the correlation coefficients between two satellites for the environments Suburban, Forest, Commercial, and Open.

4.2.2 State probability

Figure 15 shows the probabilities of the 'bad bad'-state $P_{\text{bad bad}}$ derived from the measurements and re-simulated with three channel models for the urban environment. The 'bad bad'-state is the critical system state and therefore requires a high modelling accuracy. The layout of elevation angles and azimuth separations is equal to Figure 14.

The following can be concluded from Figure 15:

- The 'bad bad'-state probability strongly depends on the elevation angles of the single satellites (cf. Figure 13). Assuming 15° elevation of two satellites, $P_{\text{bad bad}}$ is between 0.5 and 0.7 with respect to the azimuth angle separation. For the combination elevation1 = 45° and elevation2 = 15° $P_{\text{bad bad}}$ is between 0.15 and 0.25. When both satellites have 45° elevation, $P_{\text{bad bad}}$ is only between 0.05 and 0.20.
- The 'bad bad'-state probability depends further on the azimuth angle separation. It is related to the state correlation between the satellites (cf. Figure 14), whereas a low correlation coefficient results in a low 'bad bad'-state probability and provides therefore a high signal availability. A large variance due to the azimuth angle separation is seen for low elevation angles. Here, between 5° azimuth separation and about 90° azimuth separation a reduction of $P_{\text{bad bad}}$ of 20% is obtained for elevations < 30°.
- The Lutz model perfectly fits the state probabilities. This is one of the great advantages of first-order Markov chains.
- Both semi-Markov models reproduce the 'bad bad'-state probability with an accuracy of ±0.03 in general. An exception is obtained for 15° elevation of

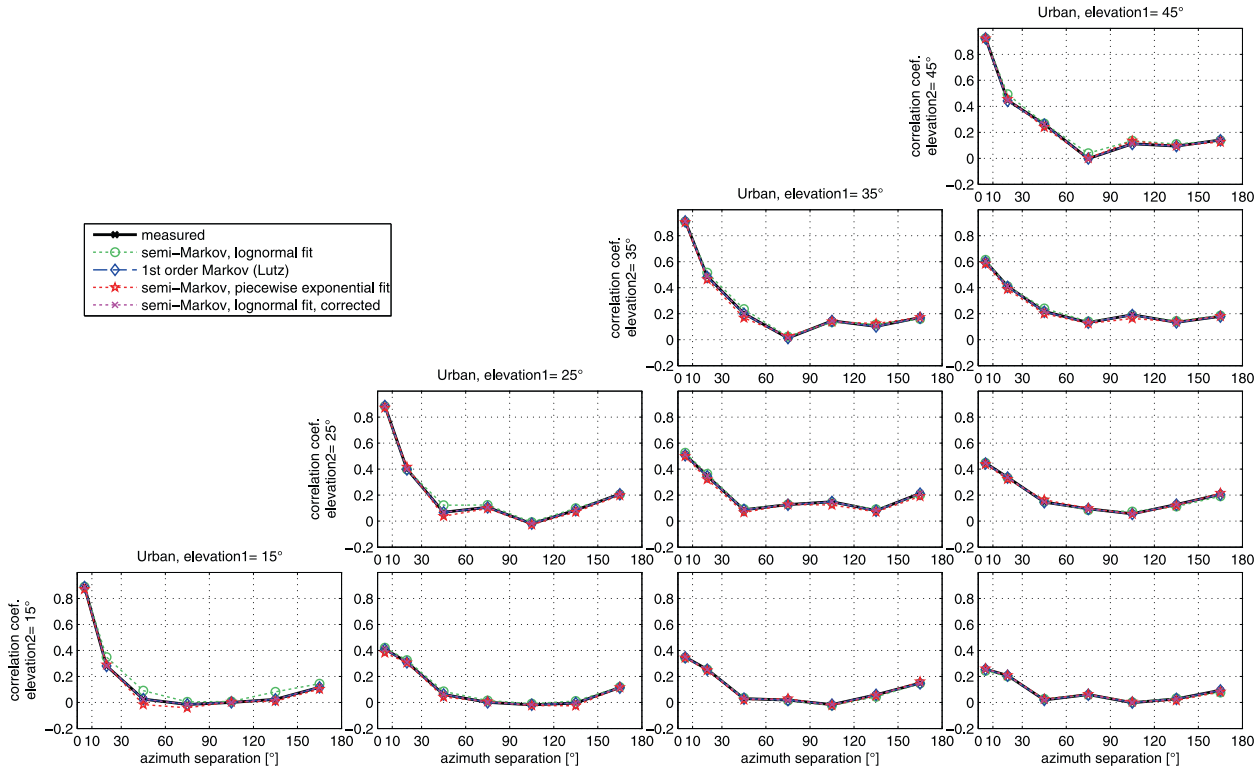

Figure 14 Correlation coefficients of the state sequences from two satellites in dependency to the azimuth separation and for different elevation angle combinations derived from the measurements and recalculated with different channel models.

both satellites, where the lognormal fit is 0.10 higher, and the piecewise exponential fit is 0.07 lower than the measured state probability.

- A correction of the lognormal fit provides an exact re-production of the state probabilities.

4.2.3 Mean state duration

The mean durations of the state 'bad bad' (no signal reception from both satellites) are given in Figure 16. The results show that in worst case (15° elevation, small azimuth separation) the mean blockage duration is up to 150 m. If only one of the satellites has a higher elevation, the mean duration of 'bad bad' is significantly lower. Values are ≈60, ≈40 and ≈20 m for elevations 25°, 35° and 45°, respectively.

From Figure 16 it is obtained that the Lutz model and the piecewise exponential curve-fit accurate describe the mean state length. For both algorithms, only a small difference between re-simulation and measurements is obtained for 15° elevation. In case of the lognormal curve fit (without correction) the mean duration is clearly overestimated for 15° elevation. The modified lognormal fit reproduces exactly the mean state duration.

4.2.4 Validation of state duration modelling

Figure 17 shows the state duration statistics for the 'bad bad'-state for the measurements and re-simulations with four state models for different elevation angles and azimuth angle separations. The quality of the curve-fits is given in Figure 18 in terms of MSEs between the measured and re-modelled SDPDF^c. From Figures 17 and 18 it can be concluded that:

- As already stated, the state durations simulated with the Lutz model (based on first-order Markov chains) follow always an exponential distribution. It is seen that the exponential distribution doesn't fit the measured state durations in an accurate manner. As seen in Figure 17, the probability of the 'bad bad'-state durations between 1 and 100 m are mainly overestimated, whereas the probability of long states above 100 m is too low. A deviation of the state duration statistic (complementary state duration CDF) up to 20% is seen between the measurements and the re-simulation with the Lutz model.
- Semi-Markov chains have high flexibility in state duration modelling. It is seen that the piecewise exponential fit as well as the lognormal fit accurately

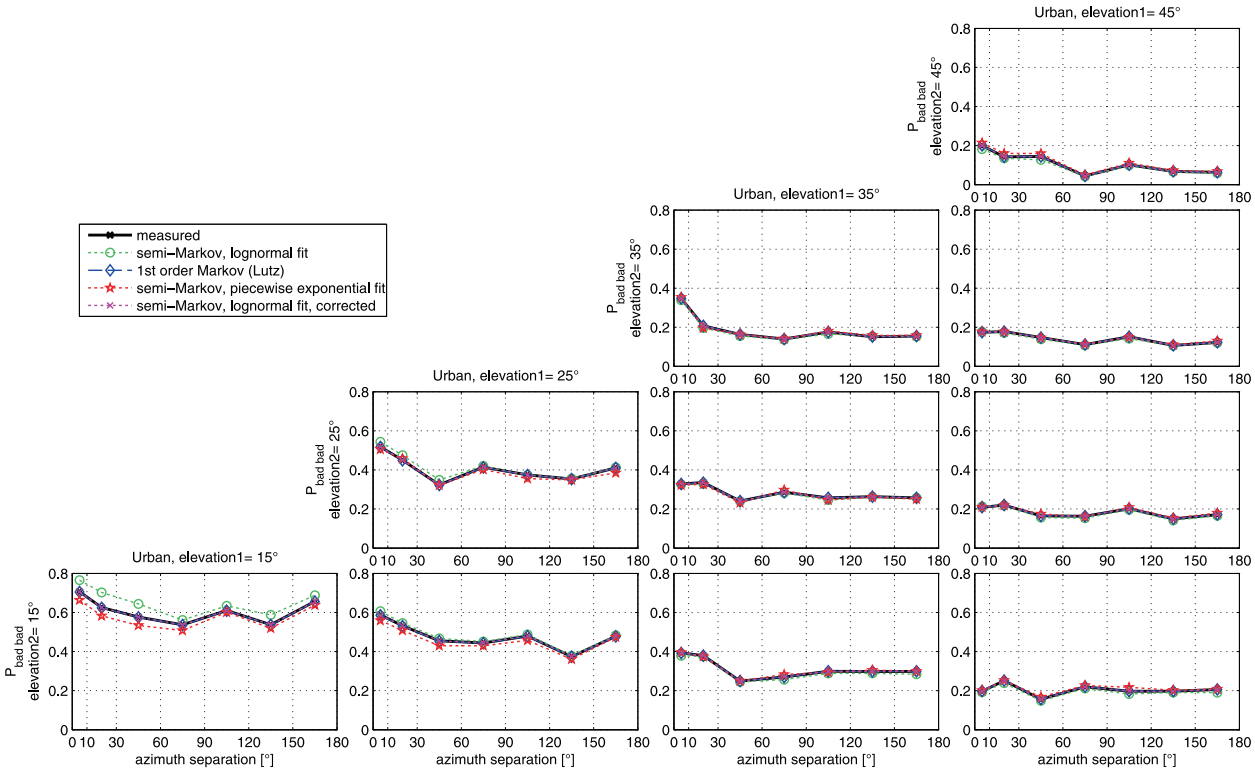

Figure 15 Probability of the 'bad bad'-state in dependency to the azimuth separation for different elevation angle combinations derived from the measurements and recalculated with different channel models.

approximate the measured state durations. The MSE values Figure 18 underline this fact.

- Although a piecewise exponential function has higher flexibility in curve-fitting, the lognormal fit provides the same good results for state duration modelling. Due to the less number of lognormal parameters per SDPDF (2 lognormal parameters instead of 11 parameters for piecewise exp. fit with 4 segments, cf. Equation (11)), it is the preferred semi-Markov approximation.

4.2.5 Conclusions on dual-satellite state modelling

For dual-satellite propagation modelling, the Lutz model is able to describe the state probabilities and average state durations exactly. It has a low complexity, since only single-satellite parameters and a correlation coefficient is needed to generate correlated state series for two satellites. A weakness is the capability of correct state duration modelling. For the optimisation of physical layer and link layer parameters for satellite broadcasting systems with high quality-of-service (QoS) requirements it has some limitations, when e.g. system blockage lengths or LOS durations are insufficiently described.

Semi-Markov models accurately describe the state durations of the dual-satellite LMS propagation channel. To reduce the complexity, two variants of SDPDF approximations were analysed: a piecewise exponential fit and a lognormal fit. The curve fits can be modified such that the state probabilities and the correlation coefficients of the measurements are exactly re-simulated. It has been shown that both the piecewise exponential fit as well as the lognormal fit describe the state duration with high accuracy. Due to the low number of required parameters, the lognormal distribution is the preferred curve fit of the SDPDF.

5 Conclusions

In this article, we compared different approaches for dual-satellite state modelling based on experimental data from different environment types, various combinations of two satellite elevation angles and different azimuth angle separations.

To find an appropriate state model architecture, the first part of this article gives a closed overview on existing state modelling approaches for single-satellite and dual-satellite reception. Three categories of models are presented: first-order Markov models, dynamic Markov models, and semi-Markov models. Based on one measurement example, a detailed analysis of diverse variants of these approaches for dual-satellite state modelling is

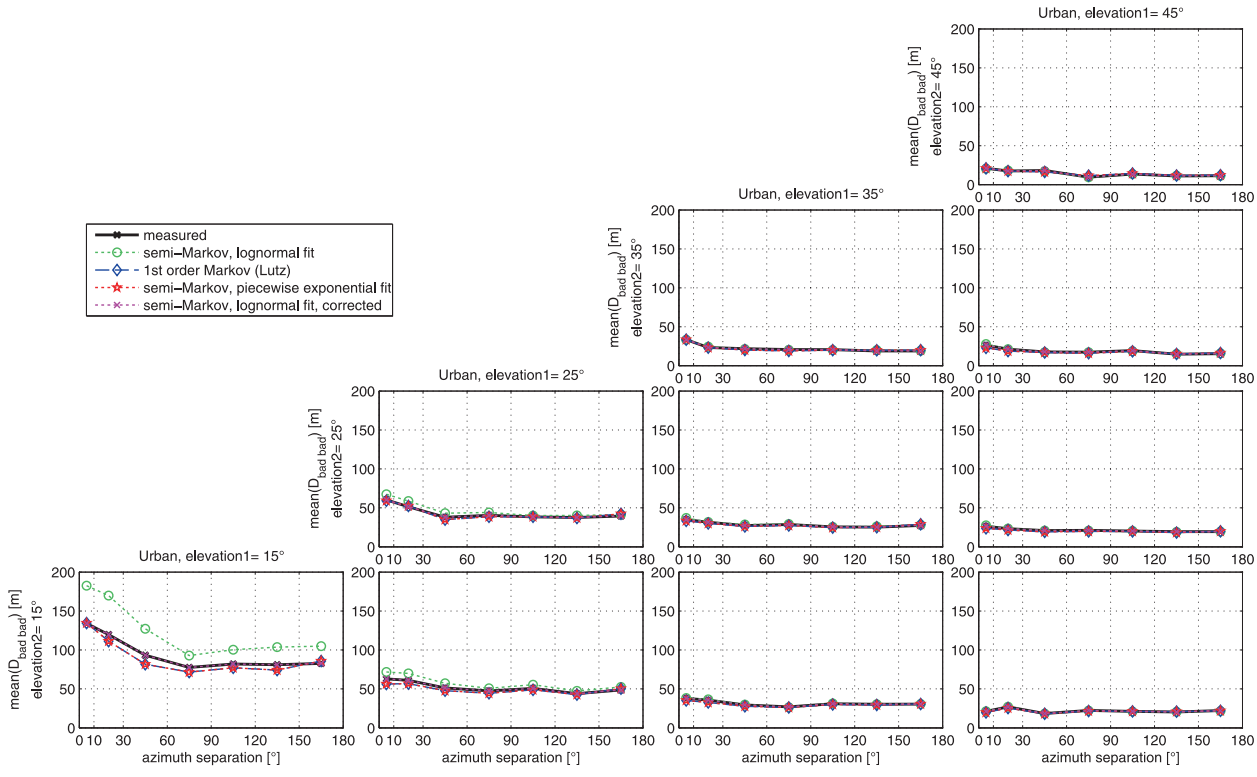

Figure 16 Mean duration of 'bad bad'-state in dependency to the azimuth separation and for different elevation angle combinations derived from the measurements and recalculated with different channel models.

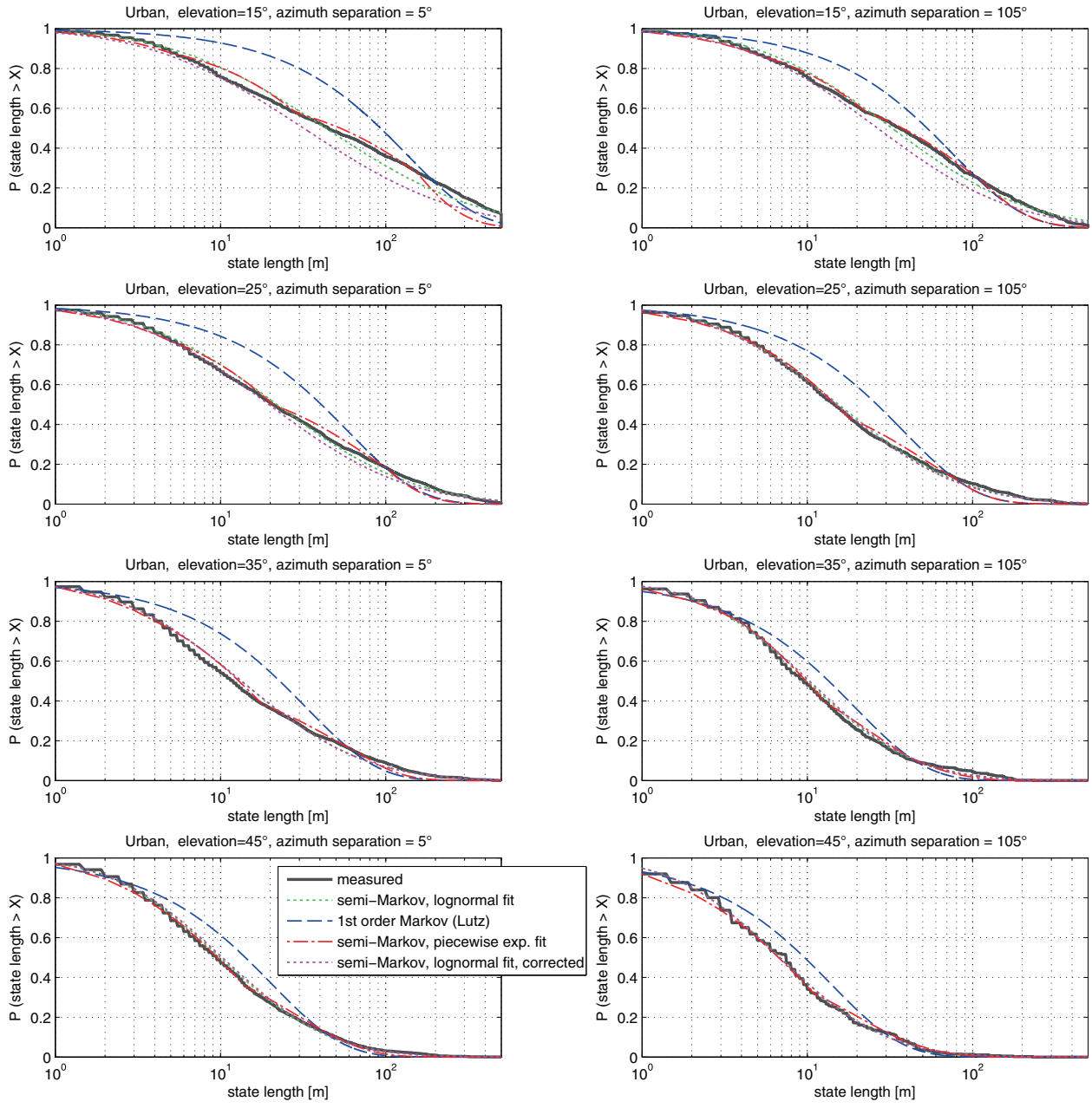

Figure 17 bad bad'-state duration statistics of the measurements and of different channel models for four elevation angles (with elevation1 = elevation2) and two azimuth angle separations in the urban environment.

performed. As evaluation criterion, the single- and dual-satellite state probabilities and the state duration statistics are compared with the measurements. Further on, the practicability of the state modelling approaches in terms of dual-satellite channel models is discussed. It was concluded that, due to the high number of required parameters and the high complexity, dynamic Markov models are not feasible in terms of dual-satellite state modelling.

In the second part of this article, three dual-satellite modelling approaches with low complexity are analysed on a large set of receive scenarios: a first-order Markov model for correlated satellites (Lutz model), a semi-Markov approach assuming a lognormal SDPDF fit, and a semi-Markov approach assuming a piecewise exponential SDPDF fit. For this purpose, the GNSS measurements are separated into various receive scenarios including five environments (urban, suburban, forest, commercial,

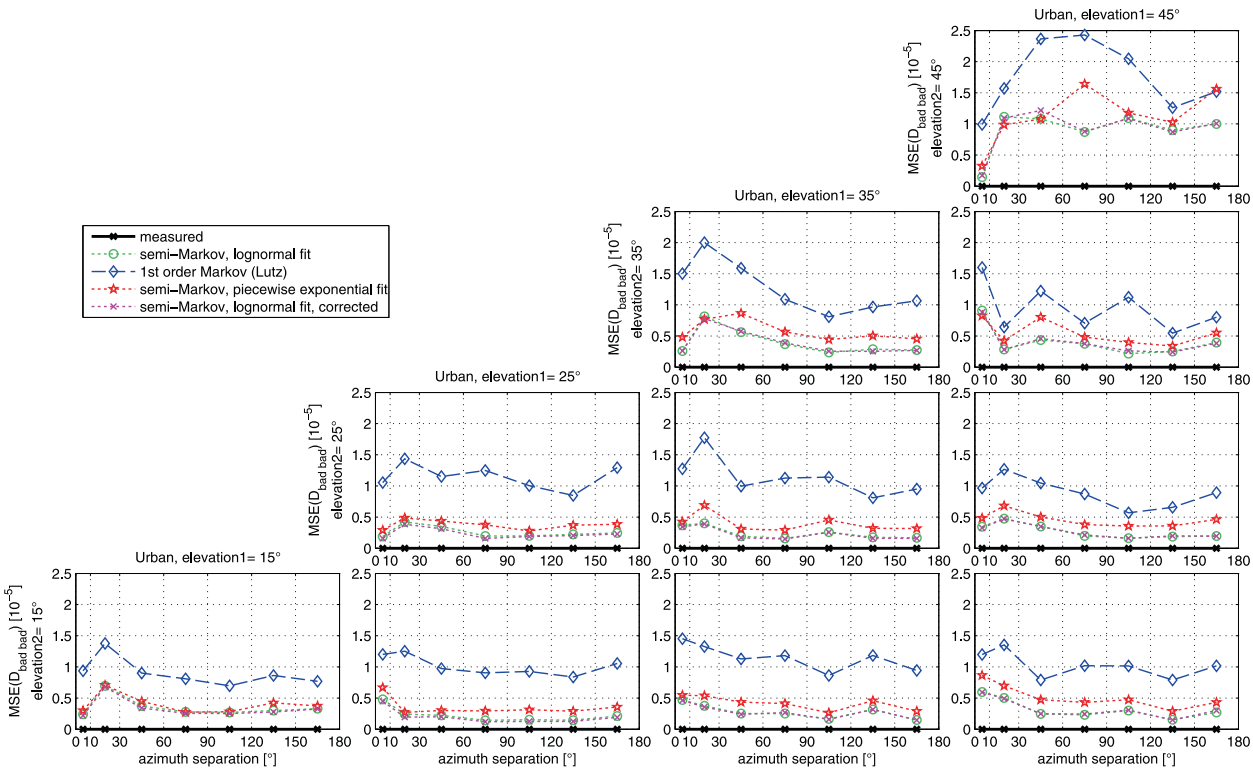

Figure 18 Evaluation of the state duration fit for the 'bad bad'-state. The Mean Squared Error (MSE) of the state duration PDF was calculated for four different state modelling approaches.

open), 8 × 8 sections with constant elevation angles of two satellites between 10° and 90°, and seven different intervals of the azimuth angle separation. Parameters for these receive scenarios has been derived for the three selected modelling approaches. Afterwards, the re-modelling results are compared with the measurements in terms of the correlation coefficient, the state probability and the state durations of the critical system state 'bad bad' in dependency on the azimuth angle separation and the elevation angles of two satellites for the urban environment. It was shown that the Lutz model accurately re-simulates the correlation coefficient and the state probability, whereas the state duration statistics are insufficiently described. The semi-Markov models describe accurately the state probabilities, the correlation coefficients, and also the state duration statistics. With respect to the number of parameters, the semi-Markov approach using a lognormal fit of the SDPDF is the preferred model for the dual-satellite state modelling and is proposed therefore for the a new dual-satellite channel model for broadcasting applications.

State parameters for the semi-Markov model as well as for the Lutz model for single- and dual-satellite reception are found in the Additional files 6, 7, 8 and 9. For the sake of completeness, we also derived Loo parameters from SDARS measurement data describing slow and fast fading effects (cf. Additional file 1). By using the two-state model according to Prieto-Cerdeira et al. [4], the parameters enable a simulation of LMS time-series for single-satellite and dual-satellite reception for different environments, elevation angles, and azimuth separations.

In the near future we will also focus on modelling of the small-scale fading. By analysing the extensive SDARS measurement data in terms of slow- and fast signal variations within MiLADY, some modifications of the two-state model from [4] are indicated. Recently, modifications were proposed in [15]. A validation of these new concepts for a multi-satellite model is topic of ongoing work.

A further task is the state analysis of multi-satellite constellations with three or more satellites. Due to the exponential growth of the model complexity with the number of satellites, new concepts must be investigated. A promising approach would be a Master–Slave concept, where several 'Slave' satellites are modelled according to their correlation with one 'Master' satellite, while neglecting the correlation between the 'Slave' satellites (cf. Section 2.4). Based on statistical parameters derived

from measurement data (such as the joint state probability for 'bad bad bad' for three satellites), the Master–Slave concept will be evaluated.

To improve the consistency of a state parameter database, activities are planned to extract state parameters with alternative methods, such as the analysis of environmental images from fish-eye cameras.

6 Endnotes

[a] The state duration statistic of a combined state include ≥ 50 elements.

[b] For single-satellite analysis only 160 segments (8 elevation angles, 5 environments and 4 driving directions) were required.

[c] Note: The MSE is estimated between measured and re-simulated state duration PDF, but the figures show the complementary CDF of the state duration for better visibility.

Additional files

Additional file 1: Two-state model parameters derived from SDARS measurements.

Additional file 2: Correlation coefficients of the state sequences from two satellites in dependency on the azimuth separation and for different elevation angle combinations derived from the measurements and recalculated with different channel models in the suburban environment.

Additional file 3: Correlation coefficients of the state sequences from two satellites in dependency on the azimuth separation and for different elevation angle combinations derived from the measurements and recalculated with different channel models in the forest environment.

Additional file 4: Correlation coefficients of the state sequences from two satellites in dependency on the azimuth separation and for different elevation angle combinations derived from the measurements and recalculated with different channel models in the commercial environment.

Additional file 5: Correlation coefficients of the state sequences from two satellites in dependency on the azimuth separation and for different elevation angle combinations derived from the measurements and recalculated with different channel models in the open environment.

Additional file 6: State parameters from SDARS measurements for a first-order Markov model and a semi-Markov model for the single-satellite reception. Each row corresponds to one receive scenario: environment, elevation, driving direction with resp. to satellite azimuth.

Additional file 7: State parameters from GNSS measurements for a first-order Markov model and a semi-Markov model for the single-satellite reception. Each row corresponds to one receive scenario: environment, elevation, driving direction with resp. to satellite azimuth.

Additional file 8: List of parameters for the semi-Markov model using a lognormal state duration PDF for dual-satellite state modelling. Each row corresponds to one receive scenario: environment, elevation of satellite 1, elevation of satellite 2, azimuth angle separation. 20 parameters per receive scenario are required: $\mu_1, \sigma_1, \ldots, \mu_4, \sigma_4$ are the parameters to describe the lognormal distribution of four joint states with the order 'good good', 'good bad', 'bad good', 'bad bad' (cf. Equation (9)); the parameters p_{ij} (with $i \neq j$ and $i, j \in 1, 2, 3, 4$) are the state transition probabilities according to the joint state transition probability matrix $\mathbf{P}_{\text{trans}}$; the state transition probabilities p_{ii} are zero.

Additional file 9: List of parameters for the Lutz model for dual-satellite state modelling. Each row corresponds to one receive scenario: environment, elevation of satellite 1, elevation of satellite 2, azimuth angle separation. The parameters for one receive scenario are a correlation coefficient and the state transition probabilities of two satellites (9 parameters).

Competing interests
The authors declare that they have no competing interests.

Acknowledgements
The GNSS and SDARS measurements were carried out in the context of the project MiLADY. This project is funded by the ARTES 5.1 Programme of the Telecommunications and Integrated Applications Directorate of the European Space Agency.

Author details
[1]Ilmenau University of Technology, Ilmenau, Germany. [2]Fraunhofer Institute for Integrated Circuits IIS, Erlangen, Germany. [3]European Space Agency, ESTEC, Noordwijk, The Netherlands.

Received: 29 November 2011 Accepted: 18 May 2012
Published: 23 July 2012

References

1. C Loo, in *ICC '84 - Links for the future: Science, systems and services for communications, Proceedings of the International Conference on Communications,* vol. 2, A statistical model for a land mobile satellite link. (Amsterdam, The Netherlands, 1984), pp. 588–594
2. E Lutz, D Cygan, M Dippold, F Dolainsky, W Papke, The land mobile satellite communication channel-Recording, statistics, and channel model, IEEE Trans. Veh. Technol. **40**, 375–386 (1991)
3. F Pérez-Fontán, M Vázquez-Castro, CE Cabado, JP Garcia, E Cubista, Statistical modeling of the LMS channel, IEEE Trans. Veh. Technol. **50**(6), 1549–1567 (2001)
4. R Prieto-Cerdeira, F Pérez-Fontán, P Burzigotti, A Bolea-Alamañac, I Sanchez-Lago, Versatile two-state land mobile satellite channel model with first application to DVB-SH analysis, Int. J. Satell. Commun. Netw. **28**, 291–315 (2010)
5. DVB BlueBook A120 (2008-05). DVB-SH Implementation Guidelines. http://www.dvb-h.org/technology.htm
6. PP Robet, BG Evans, A Ekman, Land mobile satellite communication channel model for simultaneous transmission from a land mobile terminal via two separate satellites, Int. J. Satell. Commun. **10**(3), 139–154 (1992). http://dx.doi.org/10.1002/sat.4600100304
7. E Lutz, A Markov model for correlated land mobile satellite channels, Int. J. Satell. Commun. **14**, 333–339 (1996)
8. ITU-R P.681-6, Propagation Data Required for the Design of Earth Space Land Mobile Telecommunication Systems 2003
9. M Milojević, M Haardt, E Eberlein, A Heuberger, Channel modeling for multiple satellite broadcasting systems, IEEE Trans. Broadcast. **55**(4), 705–718 (2009)
10. LE Bråten, T Tjelta, Semi-Markov multistate modeling of the land mobile propagation channel for geostationary satellites, IEEE Trans. Antennas Propag. **50**(12), 1795–1802 (2002)
11. E Eberlein, A Heuberger, T Heyn, in *ESA Workshop on Radiowave Propagation Models, Tools and Data for Space Systems,* Channel models for systems with angle diversity—the MiLADY project, (Noordwijk, The Netherlands, 2008)
12. D Arndt, A Ihlow, A Heuberger, T Heyn, E Eberlein, R Prieto-Cerdeira, in *Proceedings of the IEEE International Symposium on Broadband Multimedia Systems and Broadcasting (BMSB),* Mobile satellite broadcasting with angle diversity—performance evaluation based on measurements. (Shanghai, China, 2010), pp. 1–8
13. D Arndt, A Ihlow, A Heuberger, T Heyn, E Eberlein, in *Proceedings of the 10th Workshop Digital Broadcasting,* Land mobile satellite channel characteristics from the miLADY project. (Ilmenau, Germany, 2009), pp. 49–55

14. Corine Land cover - Technical guide. Office for official publications of the European Communities. Luxembourg. 1994
15. D Arndt, T Heyn, J König, A Ihlow, A Heuberger, R Prieto-Cerdeira, E Eberlein, in *Proceedings of the IEEE International Symposium on Broadband Multimedia Systems and Broadcasting (BMSB),* Extended two-state narrowband LMS propagation model for S-band, (Seoul, South Korea, 2012)

doi:10.1186/1687-1499-2012-228
Cite this article as: Arndt *et al.*: State modelling of the land mobile propagation channel for dual-satellite systems. *EURASIP Journal on Wireless Communications and Networking* 2012 **2012**:228.